Available online at www.sciencedirect.com
SCIENCE DIRECT®
Journal of Solid State Chemistry 178 (2005) 212–217
JOURNAL OF SOLID STATE CHEMISTRY
www.elsevier.com/locate/jssc

Synthesis, structure, band gap, and electronic structure of $CsAgSb_4S_7$

Fu Qiang Huang[a,b], James A. Ibers[a,*]

[a]Department of Chemistry, Northwestern University, 2145 Sheridan Road, Evanston, IL 60208-3113, USA
[b]Shanghai Institute of Ceramics, 1295 Dingxi Road, Shanghai 200050, China

Received 20 June 2004; received in revised form 2 October 2004; accepted 10 October 2004

Abstract

The compound $CsAgSb_4S_7$ has been synthesized by the reaction of the elements in a Cs_2S_3 flux at 773 K. The compound crystallizes in a new structure type with eight formula units in space group $C2/c$ of the monoclinic system in a cell at 153 K of dimensions $a = 26.127(2)$ Å, $b = 8.8599(7)$ Å, $c = 12.100(1)$ Å, $\beta = 97.650(1)^\circ$, and $V = 2776.0(4)$ Å^3. The structure contains two-dimensional $^2_\infty[AgSb_4S_7]$ layers separated by Cs atoms. Each $^2_\infty[AgSb_4S_7]$ layer is built from edge-sharing one-dimensional $^1_\infty[AgS_3]$ and $^1_\infty[Sb_4S_7]$ chains. Each Ag atom is tetrahedrally coordinated to four S atoms. Each Sb^{3+} center is pyramidally coordinated to three S atoms to form an SbS_3 group. $CsAgSb_4S_7$ is insulating with an optical band gap of 2.04 eV. Extended Hückel calculations indicate that the band gap in $CsAgSb_4S_7$ is dominated by the Sb 5*s* and S 3*p* states above and below the Fermi level.

Keywords: Cesium silver antimony sulfide; Crystal structure; Optical absorption spectrum; Electronic structure

1. Introduction

Silver antimony sulfides have attracted attention for a few decades owing to their interesting physical properties and potential technological applications. For example, pyrargyrite (Ag_3SbS_3) is important for nonlinear optical applications (especially optical mixing [1]). This semiconductor is transparent over a wide spectral range. It is pyroelectric and piezoelectric; it has a large refractive index and a large birefringence [2]. The formal oxidation state of Sb in Ag_3SbS_3 is 3+, consistent with the presence of pyramidal SbS_3 groups in the structure.

Recently, some alkali-metal silver antimony sulfides were synthesized by the use of supercritical ammonia as the reaction medium. These include K_2AgSbS_4 [3], Rb_2AgSbS_4 [3], α-Cs_2AgSbS_4 [4], β-Cs_2AgSbS_4 [4], KAg_2SbS_4 [3], $RbAg_2SbS_4$ [3], and $Cs_3Ag_2Sb_3S_8$ [4]. In $Cs_3Ag_2Sb_3S_8$ the formal oxidation states of the three unique Sb atoms (Sb1, Sb2, Sb3) are 3+, 3+, and 5+, whereas the formal oxidation state of Sb in the other compounds is 5+. The optical band gaps for $Cs_3Ag_2Sb_3S_8$, α-Cs_2AgSbS_4, and β-Cs_2AgSbS_4 are 2.1, 2.5, and 2.5 eV, respectively [4]. It appears that the electronic configuration of Sb affects the optical properties. However, it is not clear how the Ag 4*d*, Sb 5*s*, S 3*s*, and S 3*p* states are distributed near the Fermi level.

In order to understand the relationship between the oxidation state of Sb and the band gaps in these cesium silver antimony sulfides α-Cs_2AgSbS_4 [4], a compound of Sb^{5+}, and the new compound $CsAgSb_4S_7$, a compound of Sb^{3+}, were synthesized by the reactive flux method [5]. The crystal structure of $CsAgSb_4S_7$ was determined from single-crystal X-ray diffraction data. Optical absorption spectra were measured for α-Cs_2AgSbS_4 and $CsAgSb_4S_7$ and extended Hückel calculations were performed for these two compounds as well as for $Cs_3Ag_2Sb_3S_8$. These results are reported here.

*Corresponding author.
E-mail addresses: huangfq@mail.sic.ac.cn (F.Q. Huang), ibers@chem.northwestern.edu (J.A. Ibers).

0022-4596/$ - see front matter © 2004 Elsevier Inc. All rights reserved.
doi:10.1016/j.jssc.2004.10.014

2. Experimental section

2.1. Syntheses

The following reagents were used as obtained: Cs (Aldrich, 99.5%), Ag (Aldrich, 99.99%), Sb (Aldrich, 99.5%), and S (Alfa Aesar, 99.5%). Cs_2S_3, the reactive flux [5] employed in the syntheses, was prepared by the stoichiometric reaction of the elements in liquid NH_3. The compound α-Cs_2AgSbS_4 was synthesized by the reaction of 0.5 mmol Ag, 0.5 mmol Sb, 2.0 mmol S, and 0.5 mmol Cs_2S_3; $CsAgSb_4S_7$ was synthesized by the reaction of 0.25 mmol Ag, 1.0 mmol Sb, 2.0 mmol S, and 0.5 mmol Cs_2S_3. A reaction mixture was loaded into a fused-silica tube under an Ar atmosphere in a glove box. The tube was sealed under a 10^{-4} Torr atmosphere and then placed in a computer-controlled furnace. The sample was heated to 723 K in 6 h, kept at 723 K for 48 h, cooled at 6 K/h to 373 K, and then the furnace was turned off. The reaction mixture was washed with dimethylformamide and then stored under paraffin oil (Aldrich). The product consisted of yellow flat needles of α-Cs_2AgSbS_4 in the first reaction or red flat needles of $CsAgSb_4S_7$ in the second reaction. The yield of needles was approximately 90% (based on Ag). Examination of selected needles with an EDX-equipped Hitachi S-3500 SEM led to results consistent with the stated compositions. The compounds are unstable in air, but they can be stored under paraffin oil for months.

2.2. Structure determination of $CsAgSb_4S_7$

Single-crystal X-ray diffraction data were collected on a red flat needle of dimensions 0.042 mm × 0.080 mm × 0.130 mm with the use of graphite-monochromatized Mo$K\alpha$ radiation ($\lambda = 0.71073$ Å) at 153 K on a Bruker Smart-1000 CCD diffractometer [6]. The crystal-to-detector distance was 5.023 cm. Crystal decay was monitored by recollecting 50 initial frames at the end of the data collection. Data were collected by a scan of 0.3° in ω in four groups of 606 frames at φ settings of 0°, 90°, 180°, and 270°. The exposure time was 10 s/frame. The collection of the intensity data was carried out with the program SMART [6]. Cell refinement and data reduction were carried out with the use of the program SAINT [6] and face-indexed absorption corrections were performed numerically with the use of the program XPREP [7]. Then the program SADABS [6] was employed to make incident beam and decay corrections.

The structure was solved with the direct-methods program SHELXS and refined with the full-matrix least-squares program SHELXL of the SHELXTL suite of programs [7]. The final refinement included anisotropic displacement parameters and a secondary extinction correction. The program TIDY [8] was then employed to standardize the atomic coordinates. Additional experimental details are shown in Table 1 and in Supplementary Material. Table 2 presents selected metrical data.

2.3. UV-vis diffuse reflectance spectroscopy

A Cary 1E UV-visible spectrophotometer with a diffuse reflectance accessory was used to measure the diffuse reflectance spectra of the compounds α-Cs_2AgSbS_4 and $CsAgSb_4S_7$ (protected by thin films of paraffin oil) over the range 400 nm (3.10 eV) to 800 nm (1.55 eV) at 293 K.

Table 1
Crystal data and structure refinement for $CsAgSb_4S_7$

Formula mass	952.20
Space group	$C2/c$
a (Å)	26.127(2)
b (Å)	8.8599(7)
c (Å)	12.100(1)
β (deg)	97.650(1)
V (Å^3)	2776.0(4)
Z	8
T (K)	153(2)
λ (Å)	0.71073
ρ_c (g/cm^3)	4.557
μ (cm^{-1})	126.64
R (F)[a]	0.0285
R_w (F_o^2)[b]	0.0638

[a] $R(F) = \sum ||F_o| - |F_c|| / |F_o|$ for $F_o^2 > 2\sigma(F_o^2)$.
[b] $R_w(F_o^2) = \{\sum[w(F_o^2 - F_c^2)^2] / \sum wF_o^4\}^{1/2}$ for all data. $w^{-1} = \sigma^2(F_o^2) + (0.025 \times ((F_o^2 + 2F_c^2)/3)^2)$ for $F_o^2 \geq 0$ and $w^{-1} = \sigma^2(F_o^2)$ for $F_o^2 < 0$.

Table 2
Selected distances (Å) and angles (deg) for $CsAgSb_4S_7$

Bond	Distance	Bond	Distance or angle
Cs1–S1 × 2	3.694(1)	Ag–S5′	2.502(1)
Cs1–S2 × 2	3.681(1)	Ag–S5	2.533(1)
Cs1–S6 × 2	4.061(2)	Ag–S6	2.669(1)
Cs1–S7 × 2	3.821(1)	S1–Sb1–S4	93.21(4)
Cs2–S3 × 2	3.403(1)	S2–Sb1–S1	95.15(4)
Cs2–S4 × 2	3.813(1)	S2–Sb1–S4	93.26(4)
Cs2–S5 × 2	3.937(1)	S2–Sb2–S7	90.89(4)
Cs2–S6 × 2	3.961(1)	S6–Sb2–S2	98.86(5)
Cs2–S7 × 2	3.919(1)	S6–Sb2–S7	89.41(4)
Sb1–S1	2.476(1)	S4–Sb3–S3	95.51(4)
Sb1–S2	2.472(1)	S5–Sb3–S4	92.10(5)
Sb1–S4	2.546(1)	S5–Sb3–S3	88.97(4)
Sb2–S2	2.504(1)	S3–Sb4–S1	90.28(4)
Sb2–S6	2.422(1)	S7–Sb4–S3	102.86(5)
Sb2–S7	2.588(1)	S7–Sb4–S1	93.10(4)
Sb3–S3	2.536(1)	S5–Ag–S4	95.31(4)
Sb3–S4	2.474(1)	S5′–Ag–S4	99.00(4)
Sb3–S5	2.407(1)	S5–Ag–S6	98.05(4)
Sb4–S1	2.583(1)	S5′–Ag–S6	105.78(4)
Sb4–S3	2.440(1)	S5′–Ag–S5	137.29(3)
Sb4–S7	2.434(1)	S6–Ag–S4	125.15(4)
Ag–S4	2.864(1)		

2.4. Extended Hückel calculations

Calculations were performed for α-Cs_2AgSbS_4, $Cs_3Ag_2Sb_3S_8$, and $CsAgSb_4S_7$ by means of the tight-binding extended Hückel (EH) method [9–11]. The molecular orbital energy levels, the density of states (DOS), and the crystal orbital overlap population (COOP) curves were computed. 200 k-points in the irreducible wedge of the Brillouin zone were used in the EH computation of the DOS. The use of 500 k-points afforded the same results. The EH parameters used in the computation are listed in Table 3.

3. Results

3.1. Syntheses

The new compound $CsAgSb_4S_7$ and the known compound α-Cs_2AgSbS_4 [4] have been synthesized in greater than 90% yield from the elements in a Cs_2S_3 flux at 723 K. The composition of $CsAgSb_4S_7$ was established from the structure analysis; that α-Cs_2AgSbS_4 had been resynthesized was established from a unit-cell determination.

3.2. Crystal structure of $CsAgSb_4S_7$

This compound crystallizes in a new structure type with eight formula units in space group $C2/c$ of the monoclinic system. The crystal structure is illustrated in Fig. 1. The structure contains no metal–metal bonds and no S–S bonds so the formal oxidation states for Cs, Ag, Sb, and S in $CsAgSb_4S_7$ are as 1+, 1+, 3+, and 2−, respectively. The structure comprises $^2_\infty[AgSb_4S_7]$ layers perpendicular to [010]. The layers are separated by Cs atoms. In the structure there are two crystallographically unique Cs atoms, one unique Ag atom, and four unique Sb atoms. Atoms Cs1 (site symmetry 2) and Cs2 (site symmetry $\bar{1}$) are coordinated to eight and ten S atoms, respectively. The Ag atom is coordinated by four S atoms (S4, S5, S5′, S6) at the vertices of a distorted tetrahedron. Each Sb atom is pyramidally coordinated by three S atoms, as shown in Fig. 2. The lone pair of electrons on each Sb^{3+} center is presumably located at the fourth coordination site to complete a distorted tetrahedron. The $^2_\infty[AgSb_4S_7]$ layer comprises $^1_\infty[Sb_4S_7]$ chains (Fig. 3) linked by Ag atoms coordinated to three S atoms (S4, S5, S6) in one chain and atom S5′ in another chain. The $^1_\infty[Sb_4S_7]$ chain consists of four SbS_3 groups. The groups $Sb1S_3$, $Sb3S_3$, and $Sb4S_3$ form a distorted six-membered ring. These rings are linked with each other through an $Sb2S_3$ group. The AgS_4 tetrahedra share their vertices to form a $^1_\infty[AgS_3]$ chain (Fig. 4). In the $^2_\infty[AgSb_4S_7]$ layer, all these SbS_3 and AgS_4 polyhedra are connected by vertex-sharing.

In contrast to $CsAgSb_4S_7$, α-Cs_2AgSbS_4, β-Cs_2AgSbS_4, and $Cs_3Ag_2Sb_3S_8$ are one-dimensional structures [4]. α-Cs_2AgSbS_4 and β-Cs_2AgSbS_4 contain $^1_\infty[AgSb_4]$ chains composed of AgS_4 and SbS_4

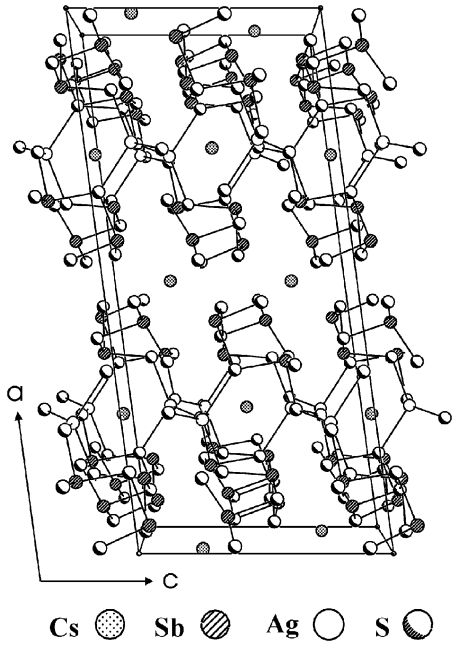

Fig. 1. The unit cell of $CsAgSb_4S_7$ viewed down [010].

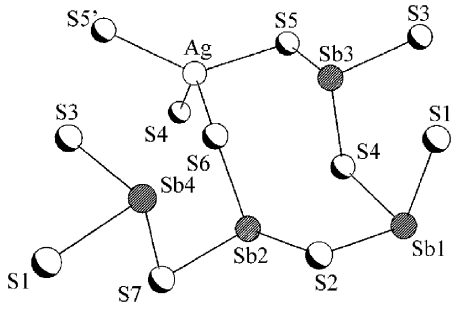

Fig. 2. The structural unit in $CsAgSb_4S_7$.

Table 3
Extended Hückel parameters

	Orbital	H_{ii} (eV)	ζ_1[a]	ζ_2	c_1[a]	c_2
Cs	6*s*	−3.88	1.5			
	6*p*	−2.49	1.5			
Ag	5*s*	−7.56	2.244			
	5*p*	−3.83	2.244			
	4*d*	−11.58	6.07	2.663	0.5889	0.637
Sb	5*s*	−18.8	2.323			
	5*p*	−11.7	1.999			
S	3*s*	−20.0	1.817			
	3*p*	−13.3	1.817			

[a]Exponents and coefficients in a double expansion of the *d* orbital.

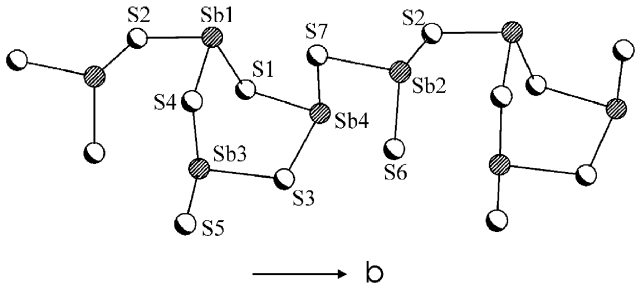

Fig. 3. The $^{1}_{\infty}[Sb_4S_7]$ chain in $CsAgSb_4S_7$.

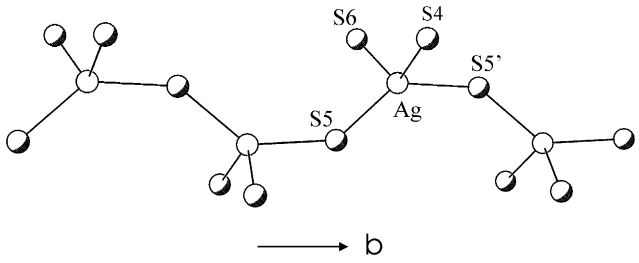

Fig. 4. The $^{1}_{\infty}[AgS_3]$ chain in $CsAgSb_4S_7$.

tetrahedra. $Cs_3Ag_2Sb_3S_8$ contains a $^{1}_{\infty}[AgSb_3S_8]$ chain comprising SbS_3 pyramids (Sb^{3+}) and AgS_4 and SbS_4 (Sb^{5+}) tetrahedra.

Selected metrical data for the $CsAgSb_4S_7$ structure are listed in Table 2. The Cs–S distances from 3.403(1) to 4.061(2) Å are in the range of those found in α-Cs_2AgSbS_4, β-Cs_2AgSbS_4, and $Cs_3Ag_2Sb_3S_8$ (3.392(4)–4.025(4) Å). The Ag–S distances of 2.502(1)–2.864(1) Å are also in the range of those of 2.472(6)–2.923(5) Å in these same compounds. The Sb^{3+}–S distances of 2.407(1)–2.588(1) Å in the SbS_3 pyramids of the present compound are comparable to those of 2.385(7)–2.497(6) Å in $Cs_3Ag_2Sb_3S_8$. As expected, these Sb^{3+}–S distances are longer than the Sb^{5+}–S distances of 2.308(9)–2.349(4) Å in the SbS_4 tetrahedra of α-Cs_2AgSbS_4, β-Cs_2AgSbS_4, and $Cs_3Ag_2Sb_3S_8$.

In the $CsAgSb_4S_7$ structure the Sb atom of each SbS_3 pyramid interacts on its lone-pair side with other S atoms at distances of 3.0–3.9 Å. These distances, which are longer than Sb–S single bonds but shorter than van der Waals' interactions, are characteristic of secondary interactions [12,13].

3.3. Optical absorption measurements

The optical absorption spectra for $CsAgSb_4S_7$ and α-Cs_2AgSbS_4 in the range 400 nm (3.10 eV) to 800 nm (1.55 eV) are shown in Fig. 5. The derived band gaps are 2.04 eV (608 nm) in $CsAgSb_4S_7$ and 2.56 eV (485 nm) in α-Cs_2AgSbS_4, consistent with their colors of yellow and red, respectively. The latter value agrees well with that of 2.5 eV obtained previously [4].

3.4. Electronic structures

The electronic structures of $CsAgSb_4S_7$, α-Cs_2AgSbS_4, and $Cs_3Ag_2Sb_3S_8$ were calculated by means of the EH method. Although this method does not provide reliable band gaps, it does yield useful information on frontier molecular orbitals, electron density distributions, partial charges, dipole moments, and bond orders. Fig. 6 shows the total DOS and the contributions from the Sb, Ag, and S atoms for $CsAgSb_4S_7$ and α-Cs_2AgSbS_4. The Cs 6*s* states are high in energy and thus are not included in the plots. As shown, there are far more occupied Sb 5*s* states in $CsAgSb_4S_7$ than in α-Cs_2AgSbS_4, consistent with the assignments of the formal oxidation states for Sb of 3+ in $CsAgSb_4S_7$ and of 5+ in α-Cs_2AgSbS_4.

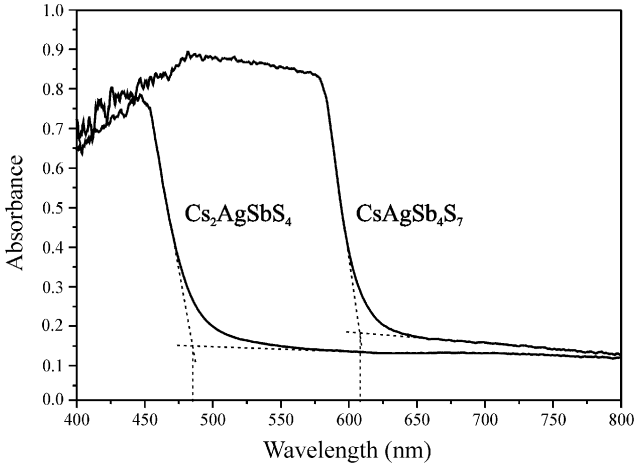

Fig. 5. Optical absorption spectra of $CsAgSb_4S_7$ and α-Cs_2AgSbS_4.

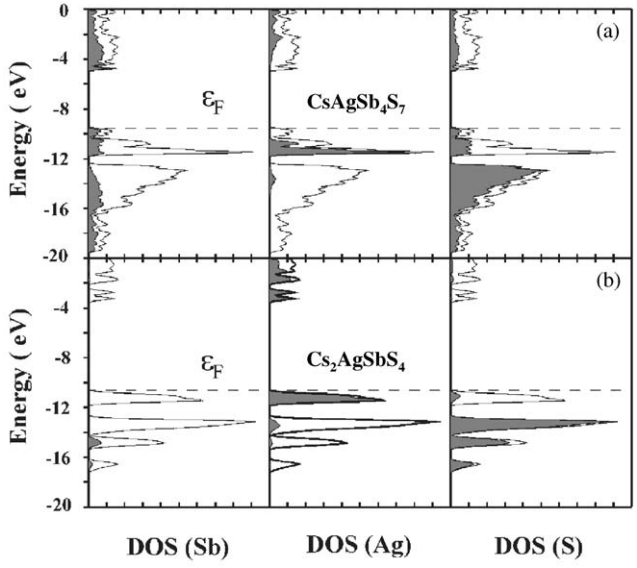

Fig. 6. The total and partial (Sb, Ag, S) DOS of (a) $CsAgSb_4S_7$, (b) and α-Cs_2AgSbS_4. The total DOS and the partial DOS (filled area) are shown in each plots.

Because the S states in $CsAgSb_4S_7$ are much less localized than in α-Cs_2AgSbS_4, the total DOS in $CsAgSb_4S_7$ is more dispersive. The Ag 4*d* states in both compounds, mainly localized between −10 and −12 eV, have weak bonding interactions with the S states. The major lowest unoccupied states are a mixture of Sb and S states in $CsAgSb_4S_7$ and a mixture of Ag and a very few S states in α-Cs_2AgSbS_4, as shown in Fig. 6. Thus, the band gaps are dominated mainly by the Sb and S states in $CsSb_4AgS_7$ and by the Ag and S states in α-Cs_2AgSbS_4.

$Cs_3Ag_2Sb_3S_8$ contains two unique Sb^{3+} atoms and one unique Sb^{5+} atom. Its DOS, calculated in a similar manner, confirms again that the Sb^{3+} states play a more important role in reducing the band gap than do the Sb^{5+} states (Fig. 7). This should also be the case in the corresponding selenides, if they can be synthesized.

The lone-pair electrons in $CsAgSb_4S_7$ and $Cs_3Ag_2Sb_3S_8$ cause the Sb 5*s* states to be near the Fermi level whereas the unoccupied Sb 5*s* states in α-Cs_2AgSbS_4 are far above the Fermi level. The experimental band gaps in $CsAgSb_4S_7$ (2.04 eV) and $Cs_3Ag_2Sb_3S_8$ (2.1 eV) arise from the presence of Sb^{3+}; the larger experimental band gap in α-Cs_2AgSbS_4 (2.56 eV) results from Ag and S states near the Fermi level.

Fig. 8 presents the COOP curves for some representative bonds in $CsAgSb_4S_7$ and α-Cs_2AgSbS_4. Note that below the Fermi level many states contribute to bonding owing to the mixing among Sb^{3+} and S states in $CsAgSb_4S_7$ and among Ag and S states in α-Cs_2AgSbS_4. The energy sequence of the three kinds of bond COOPs is Sb^{3+}–S > Ag^{+}–S > Sb^{5+}–S. As shown in Fig. 8, the occupied and unoccupied Sb^{3+}–S states are distributed much closer to the Fermi level than are the occupied and unoccupied Sb^{5+}–S states. The COOP values for the Sb^{3+}–S bonds are negative near the Fermi level. Overall, the lone-pair electrons weaken the Sb^{3+}–S bonds compared with the Sb^{5+}–S bonds, consistent with the average Sb^{3+}–S bond being longer than the Sb^{5+}–S bond.

4. Supplementary material

Crystallographic data in CIF format for $CsAgSb_4S_7$ have been deposited as CSD number 414420. These data may be obtained free of charge by contacting FIZ Karlsruhe at +49 7247 808 666 (fax) or crysdata@fiz-karlsruhe.de (email).

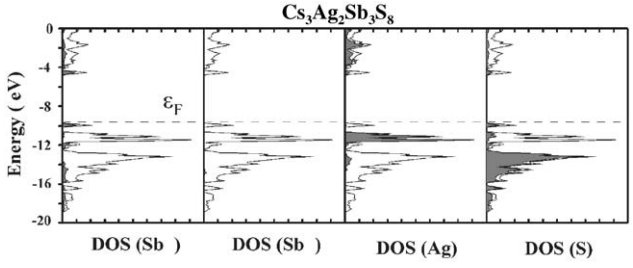

Fig. 7. The total and partial (Sb, Ag, S) DOS of $Cs_3Ag_2Sb_3S_8$. The total DOS and the partial DOS (filled area) are shown in each plots.

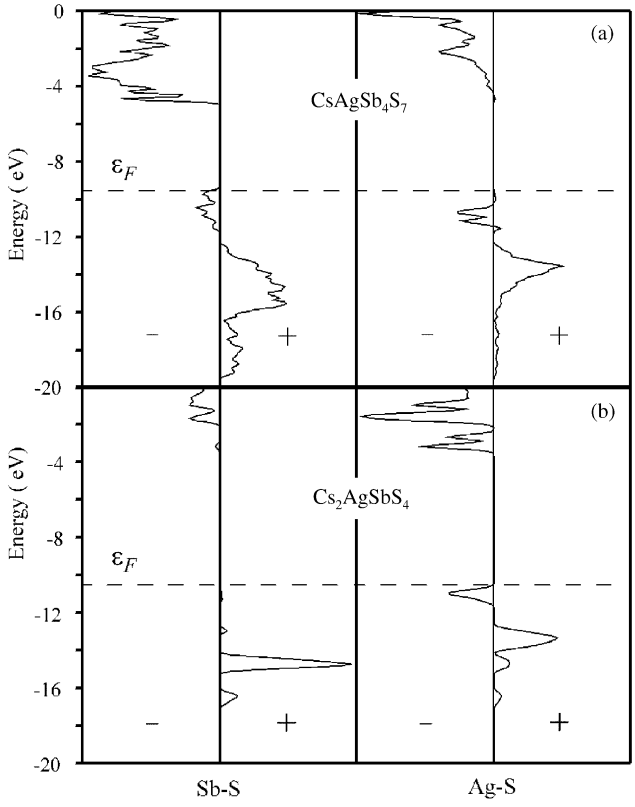

Fig. 8. EH COOP plots for representative bonds (Sb–S and Ag–S) in (a) $CsAgSb_4S_7$ and (b) α-Cs_2AgSbS_4, respectively. The + region is bonding and the − region is antibonding.

Acknowledgments

This research was supported by National Science Foundation Grant DMR00-96676. Use was made of the Central Facilities supported by the MRSEC program of the National Science Foundation (DMR00-76097) at the Materials Research Center of Northwestern University.

References

[1] H.M. Khlyap, V.I. Bilozertseva, L.N. Panchenko, European Materials Research Society Meeting, Warsaw University of Technology, 2004, poster A26.
[2] K.A. Schönau, S.A.T. Redfern, J. Appl. Phys. 92 (2002) 7415–7424.
[3] G.L. Schimek, W.T. Pennington, P.T. Wood, J.W. Kolis, J. Solid State Chem. 123 (1996) 277–284.
[4] P.T. Wood, G.L. Schimek, J.W. Kolis, Chem. Mater. 8 (1996) 721–726.

[5] S.A. Sunshine, D. Kang, J.A. Ibers, J. Am. Chem. Soc. 109 (1987) 6202–6204.
[6] Bruker, SMART Version 5.054 Data Collection and SAINT-Plus Version 6.45a Data Processing Software for the SMART System, 2003 (Bruker Analytical X-ray Instruments, Inc., Madison, WI, USA).
[7] G.M. Sheldrick, SHELXTL DOS/Windows/NT Version 6.14, 2003 (Bruker Analytical X-ray Instruments, Inc., Madison, WI, USA).
[8] L.M. Gelato, E. Parthé, J. Appl. Crystallogr. 20 (1987) 139–143.
[9] G. Landrum, Yet Another Extended Hückel Molecular Orbital Package (YAeHMOP) Version 2.0, 1997.
[10] R. Hoffmann, J. Chem. Phys. 39 (1963) 1397–1412.
[11] M.-H. Whangbo, R. Hoffmann, J. Am. Chem. Soc. 100 (1978) 6093–6098.
[12] N.W. Alcock, Adv. Inorg. Chem. Radiochem. 15 (1972) 1–58.
[13] A.J. Barton, N.J. Hill, W. Levason, B. Patel, G. Reid, Chem. Commun. (2001) 95–96.